

Electromagnetic modeling and performance comparison of different pad-to-pad length ratio for dynamic inductive power transfer

Original

Electromagnetic modeling and performance comparison of different pad-to-pad length ratio for dynamic inductive power transfer / Cirimele, Vincenzo; Pichon, Lionel; Freschi, Fabio. - ELETTRONICO. - (2016), pp. 4499-4503. (Intervento presentato al convegno Industrial Electronics Society , IECON 2016 - 42nd Annual Conference of the IEEE tenutosi a Firenze, ITA nel 23-26 ottobre 2016) [10.1109/IECON.2016.7793667].

Availability:

This version is available at: 11583/2661187 since: 2020-01-23T16:29:54Z

Publisher:

IEEE

Published

DOI:10.1109/IECON.2016.7793667

Terms of use:

This article is made available under terms and conditions as specified in the corresponding bibliographic description in the repository

Publisher copyright

IEEE postprint/Author's Accepted Manuscript

©2016 IEEE. Personal use of this material is permitted. Permission from IEEE must be obtained for all other uses, in any current or future media, including reprinting/republishing this material for advertising or promotional purposes, creating new collecting works, for resale or lists, or reuse of any copyrighted component of this work in other works.

(Article begins on next page)

Electromagnetic modeling and performance comparison of different pad-to-pad length ratio for dynamic Inductive Power Transfer

Vincenzo Cirimele^{1,2}, Lionel Pichon², Fabio Freschi¹

¹Politecnico di Torino, Department of Energy
Corso Duca degli Abruzzi, 24, 10129, Torino, Italy

²GeePs — Group of electrical engineering - Paris, UMR CNRS 8507,
CentraleSupélec, Univ. Paris-Sud, Université Paris-Saclay, Sorbonne Universités, UPMC Univ Paris 06
3 & 11 rue Joliot-Curie, Plateau de Moulon 91192 Gif-sur-Yvette CEDEX, France
Email: vincenzo.cirimele@polito.it

Abstract—Several recent research efforts are oriented towards the dynamic inductive power transfer for the charge of electric vehicles during their motion. This possibility presents several open issues that need a solution. The present paper focuses on the analysis of the effects related to the variation of the ratio between the transmitter and the receiver pad lengths with respect to a basic case in which the two pads have the same dimensions. Three cases are analyzed by means of an accurate electromagnetic modeling investigating the power transfer characteristics and the induced losses in the vehicle chassis.

Index Terms—Electric vehicles - Inductive power transmission - Electromagnetic modeling - Finite element method

I. INTRODUCTION

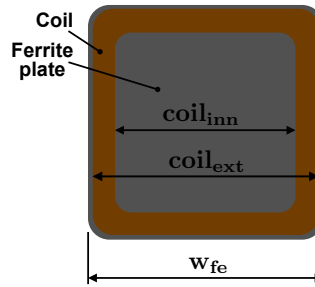
The inductive power transfer (IPT) for electric vehicles is becoming an industrial-ready technology. The IPT is essentially based on the resonance of two magnetically coupled inductors, one placed on or under the ground, usually named transmitter, and a second one, named receiver, placed under the vehicle floor. This system allows the transfer of electrical energy to the vehicle in absence of physical contacts introducing a series of advantages as the start of the charge operations without any human action, the consequent improvement of the safety and the absence of external installations that means a strong reduction of possible damages or acts of vandalism.

Several works [1]–[8] in the last decade, demonstrated the feasibility and the good efficiency of *static IPT* systems that operates with the vehicles stopped over a charging station with fixed alignment and coupling between the two coils. Recently, the interest of researchers is focused on the *dynamic IPT* or rather, the extension of the IPT technology towards its use during the vehicle motion. The success of these studies could lead toward a strong reduction of the battery capacity installed on board together with the elimination of the necessity of stops for the charge, contributing to the acceptance and diffusion of electric mobility.

However, while the static IPT has been deeply investigated and a related standardization process is already ongoing [9]–[11], only few works demonstrated the effectiveness of dynamic IPT systems [12]–[15]. This points out as dynamic

TABLE I: Physical dimensions of the basic pad.

| Parameter | Value |
|---------------------------------------|--------|
| Ferrite plate width (w_{fe}) | 0.6 m |
| Ferrite plate thickness (th_{fe}) | 5 mm |
| Coil external width ($coil_{ext}$) | 0.58 m |
| Coil inner width ($coil_{inn}$) | 0.38 m |
| Wire diameter (d_{wire}) | 5 mm |
| Number of turns (N) | 8 |

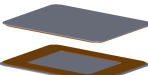
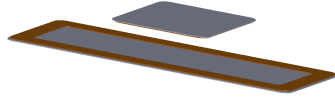
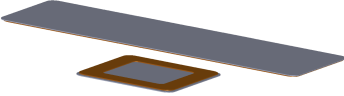


IPT presents several open issues that need to be deeply investigated. An important example is represented by the shape of transmitter and receiver magnetic structures. Like for the static solutions, there is not a clear and univocal direction with respect to this issue. The Korea Advanced Institute of Science & Technology (KAIST) is continuing to move in the direction of long transmitter tracks in the order of hundred meters [16] while the Oak Ridge National Laboratory (ORNL) and the team of the Auckland University propose the use of small pads of the same dimension on both sides [13], [17]. Recently, the researchers of CIRCE laboratory in Spain proposed to adopt a receiver longer than the transmitter [18]. Each solution differs in terms of basic shape, circular or squared, wires disposition and materials. This paper focuses on the issue of the pad shape, investigating the influence of the variation of the ratio between the receiver and the transmitter length with respect to the behavior of the coupling and the related effect on the induced losses in the vehicle chassis.

II. SYSTEM DESCRIPTION

The basic pads adopted for the evaluation are a couple of identical unipolar squared pads similar to those proposed in

TABLE II: Analyzed pads configurations

| Name | Pads aspect | Transmitter to receiver length ratio |
|-------|---|--------------------------------------|
| EQUAL |  | 1:1 |
| TRx3 |  | 3:1 |
| REx3 |  | 1:3 |

[8] and whose dimensions are reported in Table I. The pads are made of a copper coil and a plate of ferrite with relative permeability $\mu_r = 2000$. The distance between the coils is fixed at 20 cm. A metallic plate of dimension 1.8×4 m is placed at 25 cm above the transmitter. This plate models the floor of the vehicle chassis of a typical compact or family car [19]. It is made of a steel with conductivity $\sigma = 10$ MS/m and relative permeability $\mu_r = 200$. The layout of the system is depicted in Fig. 1.

Starting from the basic pad, other two configurations are derived by modifying only the dimension along the y axis considered as the length of the coil. Each derived configuration is obtained by multiplying three times the length of only one basic pad leaving unchanged the other one. The resulting couples are illustrated in Table II.

III. ELECTROMAGNETIC MODELING

The simulation of the system is conducted using the finite element method. In order to provide an accurate evaluation of the parameters of interest, particular attention is posed on the modeling of the coils and the vehicle chassis.

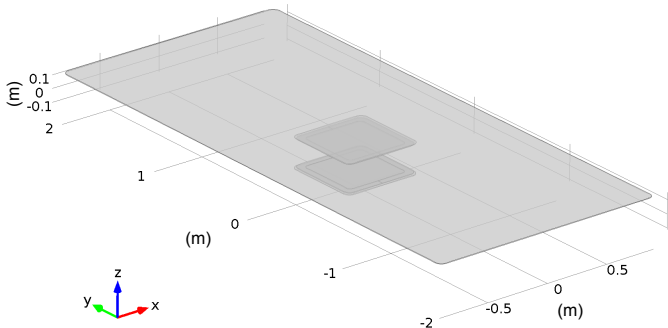


Fig. 1: 3D representation of the system of the basic pads and the plate representing the vehicle floor.

The coils are treated as ideal massive coils [20] having height equal to d_{wire} and width equal $N \times d_{wire}$. The mutual inductance M is calculated through the integral (1) over the volume of the receiver Ω_{re} as:

$$M = \int_{\Omega_{re}} \frac{\vec{A}_{re} \cdot \vec{J}_{re}}{I_{tr} I_{re}} d\Omega_{re} \quad (1)$$

\vec{A}_{re} is the component of the vector potential produced by the transmitter, \vec{J}_{re} is the current density in the receiver and I_{tr} and I_{re} are the current in the transmitter and receiver respectively.

Differently from previous works [21], [22] where the chassis was modeled as lossless, in this work, the chassis is treated applying the *surface impedance boundary conditions (SIBC)* [23]. This formulation approximates the penetration of the magnetic field in the inner part of the material avoiding to include its domain in the model reducing the calculation efforts. As for the perfect conductor condition, the application of the SIBC means to assume that the induced currents flow entirely on the surface of the material but, differently from the first condition, it takes into account the finite value of conductivity and permeability of the material. This offers the possibility to evaluate the induced losses P_{loss} through an integral over the chassis surface S_{ch} as:

$$P_{loss} = \frac{1}{2} \delta \int_{S_{ch}} \vec{J} \cdot \vec{E}^* dS \quad (2)$$

δ is the penetration depth defined as

$$\delta = \sqrt{\frac{2}{\omega \mu \sigma}} \quad (3)$$

while \vec{J} and \vec{E} are the current density and the electric field evaluated on the chassis boundaries.

Lastly, the ferrite is considered linear according to the dimension of the plate and the typical low level of magnetic flux density of these applications [22]. The ferrite losses are neglected according to the negligible conductivity of the ferrite (typically in the order of 10^{-12} S/m) with respect to the others materials of the model.

IV. PERFORMANCE EVALUATION

The goal of the evaluation is to compare the typical behavior during the movement of each pad configuration and compute the different effects in terms of induced losses in the chassis.

The analysis is performed in two steps. The first one is aimed to evaluate the behavior of the mutual inductance with respect to the variation of the position of the receiver pad during the vehicle movement. This information is used to evaluate the quantity of energy delivered by each pads configuration. In the second step the power losses in the chassis are evaluated considering an entire charging process. The evaluation is conducted assuming a constant speed of the vehicle in order to obtain a linear relationship between space and time.

A. Transferred energy

Considering the condition of perfect alignment of the two pads as zero reference for the position, the receiver is translated evaluating the value of the mutual inductance in each position. The resulting behaviors are depicted in Fig. 2. The position is indicated as relative misalignment with respect to the dimension of the pad which length remains equal to the basic pad (Table I). The TRx3 and REx3 configurations present

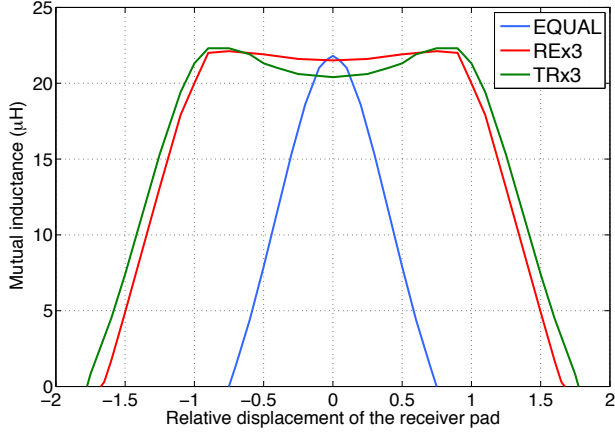


Fig. 2: Variation of the mutual inductance respect to the relative displacement of the receiver.

a stable coupling for a larger relative displacement than the EQUAL and, as a consequence, more energy delivered to the receiver. To compensate for this difference, two transmitters are added to equalize the total coil areas with respect to the configurations having longer pads. The additional pads are placed in order to obtain a unique point of null coupling that happens for a displacement of 0.75 times the pad length (Fig. 2). The resulting layout is shown in Fig. 3 while the effect on the mutual inductance is shown in Fig. 4.

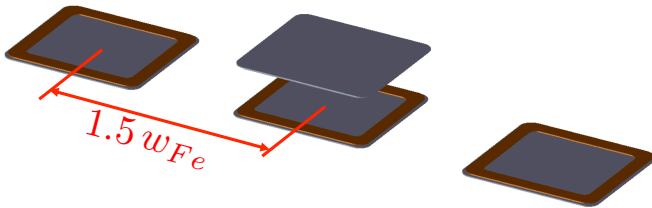


Fig. 3: EQUAL configuration with the introduction of two additional transmitter pads.

In the proposed analysis, the systems are supposed as working with a fixed sinusoidal current $i_{tr}(t)$ with 40 A rms on the transmitter side and with a fixed frequency $f_0 = 85$ kHz adopting a series-series topology for the capacitive compensation of the self-inductances of the coils as done in previously proposed solutions for dynamic IPT [12]–[15], [24]. The system can be represented through the circuit model depicted in Fig. 5 where L_{tr} and L_{re} are the self-inductances of transmitter and receiver

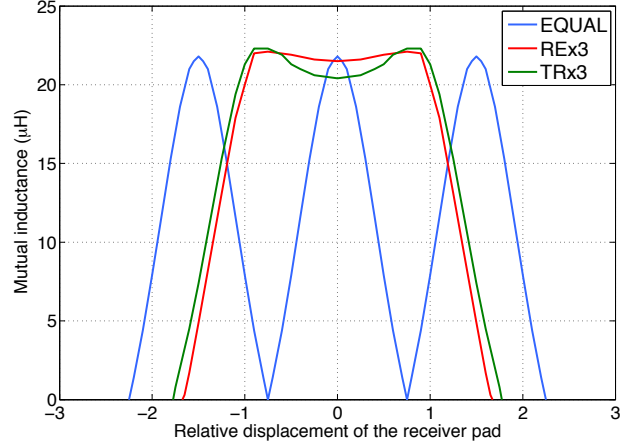


Fig. 4: Variation of the mutual inductance with respect to the relative displacement of the receiver in presence of two additional transmitters in the EQUAL configuration.

coils whose impedances at the resonance frequency are totally compensated by the capacitances C_{tr} and C_{re} respectively.

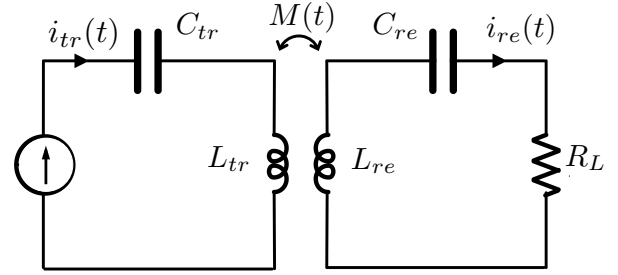


Fig. 5: Circuit representation of the analyzed configurations.

The series-series compensation topology allows to consider the condition of resonance of the system as independent of the variation of the coupling and the value of the current on the receiver as uniquely dependent on the mutual inductance [25], [26]. The load connected to the receiver is a resistor R_L whose value is assumed constant through the charging process.

Being the mutual inductance dependent on the time, it is indicated as $M(t)$. Therefore, the induced voltage $v_{oc}(t)$ at the receiver terminals can be expressed as:

$$v_{oc}(t) = M(t) \frac{di_{tr}(t)}{dt} + i_{tr}(t) \frac{dM(t)}{dt} \quad (4)$$

According to the series-series compensation topology, the induced current in the receiver is expressed as:

$$i_{re}(t) = \frac{v_{oc}(t)}{R_L} = \frac{1}{R_L} \left(M(t) \frac{di_{tr}(t)}{dt} + i_{tr}(t) \frac{dM(t)}{dt} \right) \quad (5)$$

By integrating the power delivered to the battery over the time interval required for the charging process, it is possible to evaluate the amount of transferred active energy as:

$$E_{tr} = \int_{t_i}^{t_f} \frac{1}{R_L} \left(M(t) \frac{di_{tr}(t)}{dt} + i_{tr}(t) \frac{dM(t)}{dt} \right)^2 dt \quad (6)$$

The resulted values are reported in Table III.

The comparison of the transferred energies indicates that the TRx3 and REx3 configurations are able to deliver a slightly bigger amount of energy than the EQUAL configuration (about 10 and 5% more respectively). The ratios between the energy transmitted by the EQUAL configuration respect to the one transferred in the other two cases define the *energy correction coefficients* k_{REx3} and k_{TRx3} :

$$k_{TRx3} = \frac{E_{tr} \text{ EQUAL conf.}}{E_{tr} \text{ TRx3 conf.}} = 0.91 \quad (7)$$

$$k_{REx3} = \frac{E_{tr} \text{ EQUAL conf.}}{E_{tr} \text{ REx3 conf.}} = 0.95 \quad (8)$$

B. Induced losses

To calculate the power losses, the same 40 A rms current is imposed on the transmitter while the value of the current in the receiver is calculated for each step according to (5). For each position the power losses over the chassis are evaluated through the (2). The resulting behavior of the losses during the charge process is shown in Fig. 6.

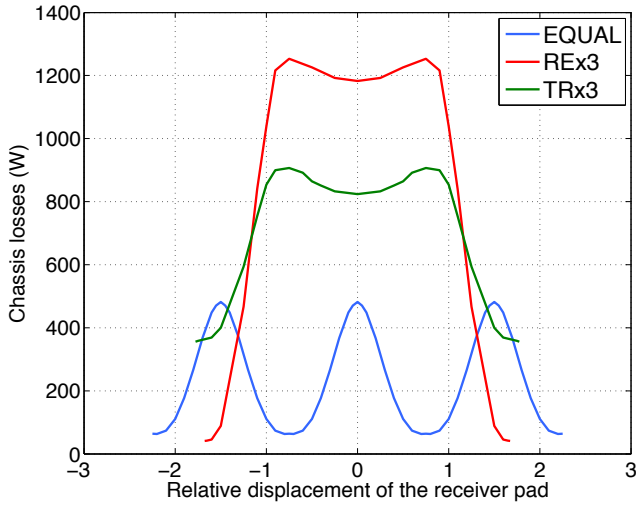


Fig. 6: Behavior of the power losses in the vehicle chassis during the motion of the charging vehicle.

The power losses are integrated with respect to time to obtain the energy dissipated during the charging processes. For the TRx3 and REx3 configurations, the value of the dissipated energy is multiplied by the corresponding energy coefficient (7) and (8). This operation means to compensate the different amounts of energy effectively transferred by the three configurations allowing to compare the different solutions considering them as delivering the same amount of energy. The results are shown in Fig. 7 while the values of transferred

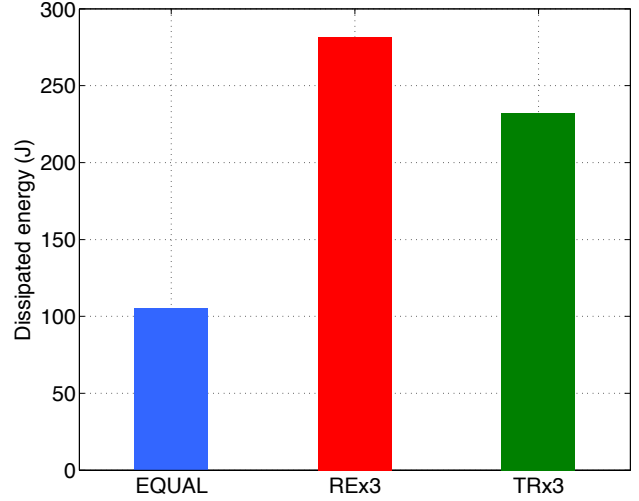


Fig. 7: Energy dissipated in the chassis during the motion of the charging vehicle for a constant speed of 40 km/h.

TABLE III: Transferred energy and efficiency of the charging process.

| | EQUAL | REx3 | TRx3 |
|---|---------|---------|---------|
| Transferred energy (E_{tr}) | 4.33 kJ | 4.76 kJ | 4.58 kJ |
| Efficiency | 97.6% | 93.8% | 94.4% |

energy and efficiency of the charging process are summarized in Table III.

V. CONCLUSIONS

This work has illustrated an effective way to model the different elements of the magnetic structure of an IPT system and has suggested the application of the SIBC formulation to the vehicle chassis. This method has allowed to study the induced losses on the model of the vehicle chassis, differently from previously proposed works which treated this component as lossless. As this method does not require any increase in the mesh elements number, it does not require any increase in the computational efforts. This technique has been adopted in the investigation of the effects of the length ratio of the pads in a dynamic IPT application.

The results derived in Section IV-A point out a difference in the way the power is delivered in the three configurations. The REx3 and TRx3 present a long interval at high level coupling meaning a stable and more constant power transfer. On the other side the EQUAL configuration is able to deliver the full power only for a very short period and the power transfer results not continuous.

The configuration TRx3 presents a small decrease of the coupling (about 1 μ H) in the aligned condition caused by the chassis. The eddy currents, in fact, create a reaction magnetic field that decreases the magnetic flux linked to the receiver. In the case of the configuration REx3, this effect is largely compensated by the larger ferrite plate on the receiver side that drives the magnetic field through the receiver.

TABLE IV: Qualitative performances of the evaluated pad configurations for equal pads area.

| | EQUAL | REx3 | TRx3 |
|---|-------|------|------|
| Efficiency for equal transferred energy | ●●● | ●○○ | ●○○ |
| Period at constant transferred power | ●○○ | ●●● | ●●● |
| Cost on vehicle side (receiver) | ●○○ | ●●● | ●○○ |
| Cost on ground side (transmitter) | ●●● | ●○○ | ●●● |

According to the results Section IV-B, both REx3 and TRx3 configurations appear less efficient than the EQUAL one. This happens according to the increased length of the coils that illuminate the chassis increasing the surface affected by the circulation of induced currents. In the TRx3 solution, the power losses are lower in accordance to the increased distance of the longer coil from the chassis that implies a lower value of the incident magnetic field.

These results suggest that the adoption of REx3 or TRx3 configuration requires an improvement of the design with the insertion of a proper good conductive material, e.g. aluminum, in order to decrease the quantity of leakage flux directed towards the chassis.

Naturally, the analysis carried out in this paper does not include all the aspects useful for a global comparison of the three analyzed configuration as the presence of an active regulation of the received power or the distribution of costs among the road infrastructure and the vehicle. Nevertheless it provides some useful indications about the general behavior of a dynamic IPT system with respect to different pad-to-pad length ratio indicating the aspects that have to be taken into account for the design. Table IV proposes a qualitative synthesis of these different aspects that will be the object of future more exhaustive works.

REFERENCES

- [1] G. Covic, J. T. Boys, *et al.*, "Inductive power transfer," *Proceedings of the IEEE*, vol. 101, no. 6, pp. 1276–1289, 2013.
- [2] M. Budhia, G. A. Covic, and J. T. Boys, "Design and optimization of circular magnetic structures for lumped inductive power transfer systems," *IEEE Transactions on Power Electronics*, vol. 26, pp. 3096–3108, Nov 2011.
- [3] H. H. Wu, A. Gilchrist, K. D. Sealy, and D. Bronson, "A high efficiency 5 kW inductive charger for evs using dual side control," *IEEE Transactions on Industrial Informatics*, vol. 8, pp. 585–595, Aug 2012.
- [4] S. Li and C. Mi, "Wireless power transfer for electric vehicle applications," *Emerging and Selected Topics in Power Electronics, IEEE Journal of*, vol. 3, pp. 4–17, March 2015.
- [5] S. Li, W. Li, J. Deng, T. D. Nguyen, and C. C. Mi, "A double-sided LCC compensation network and its tuning method for wireless power transfer," *IEEE Transactions on Vehicular Technology*, vol. 64, no. 6, pp. 2261–2273, 2015.
- [6] A. Pevere, R. Petrella, C. C. Mi, and S. Zhou, "Design of a high efficiency 22 kW wireless power transfer system for EVs fast contactless charging stations," in *Electric Vehicle Conference (IEVC), 2014 IEEE International*, pp. 1–7, 2014.

- [7] X. d. T. Garca, J. Vzquez, and P. Roncero-Snchez, "Design, implementation issues and performance of an inductive power transfer system for electric vehicle chargers with series-series compensation," *IET Power Electronics*, vol. 8, no. 10, pp. 1920–1930, 2015.
- [8] M. Ibrahim, L. Bernard, L. Pichon, E. Laboure, A. Razek, O. Cayol, D. Ladas, and J. Irving, "Inductive charger for electric vehicle: Advanced modeling and interoperability analysis," *Power Electronics, IEEE Transactions on*, vol. PP, no. 99, 2016.
- [9] J. Taiber, "Electric vehicle wireless power transfer," *Industry connections activity initiation document (ICAID). Version*, vol. 1, p. 12, 2013.
- [10] A. Gil and J. Taiber, "A literature review in dynamic wireless power transfer for electric vehicles: Technology and infrastructure integration challenges," in *Sustainable Automotive Technologies 2013*, pp. 289–298, Springer, 2014.
- [11] C. Kalialakis and A. Georgiadis, "The regulatory framework for wireless power transfer systems," *Wireless Power Transfer*, vol. 1, no. 02, pp. 108–118, 2014.
- [12] J. Huh, S. W. Lee, W. Y. Lee, G. H. Cho, and C. T. Rim, "Narrow-width inductive power transfer system for online electrical vehicles," *IEEE Transactions on Power Electronics*, vol. 26, pp. 3666–3679, Dec 2011.
- [13] O. C. Onar, J. M. Miller, S. L. Campbell, C. Coomer, C. White, and L. E. Seiber, "A novel wireless power transfer for in-motion EV/PHEV charging," in *Applied Power Electronics Conference and Exposition (APEC), 2013 Twenty-Eighth Annual IEEE*, pp. 3073–3080, 2013.
- [14] J. Shin, S. Shin, Y. Kim, S. Ahn, S. Lee, G. Jung, S.-J. Jeon, and D.-H. Cho, "Design and implementation of shaped magnetic-resonance-based wireless power transfer system for roadway-powered moving electric vehicles," *Industrial Electronics, IEEE Transactions on*, vol. 61, no. 3, pp. 1179–1192, 2014.
- [15] A. Caillierez, P. A. Gori, D. Sadarnac, A. Jaafari, and S. Loudot, "2.4 kW prototype of on-road wireless power transfer: Modeling concepts and practical implementation," in *Power Electronics and Applications (EPE'15 ECCE-Europe), 2015 17th European Conference on*, pp. 1–9, Sept 2015.
- [16] S. Choi, J. Huh, W. Lee, S. Lee, and C. Rim, "New cross-segmented power supply rails for roadway-powered electric vehicles," *Power Electronics, IEEE Transactions on*, vol. 28, no. 12, pp. 5832–5841, 2013.
- [17] G. Covic and J. Boys, "Modern trends in inductive power transfer for transportation applications," *Emerging and Selected Topics in Power Electronics, IEEE Journal of*, vol. 1, pp. 28–41, March 2013.
- [18] J. Villa, J. Sanz, J. Peri, and R. Acerete, "Victoria project: Static and dynamic wireless charging for electric buses," in *Business Intelligence on Emerging Technologies IDTechEX Conference, Berlin*, 2016.
- [19] <http://www.automobiledimension.com/>. Accessed in march 2016.
- [20] S. Babic, C. Akyel, and S. Salon, "New procedures for calculating the mutual inductance of the system: filamentary circular coil-massive circular solenoid," *Magnetics, IEEE Transactions on*, vol. 39, pp. 1131–1134, May 2003.
- [21] W. Zhang, J. White, A. Abraham, and C. Mi, "Loosely coupled transformer structure and interoperability study for EV wireless charging systems," *Power Electronics, IEEE Transactions on*, vol. 30, no. 11, pp. 6356–6367, 2015.
- [22] M. Ibrahim, L. Pichon, L. Bernard, A. Razek, J. Houivet, and O. Cayol, "Advanced modeling of a 2-kW series-series resonating inductive charger for real electric vehicle," *Vehicular Technology, IEEE Transactions on*, vol. 64, no. 2, pp. 421–430, 2015.
- [23] V. Cirimele, F. Freschi, L. Giaccone, and M. Repetto, "Finite formulation of surface impedance boundary conditions," *Magnetics, IEEE Transactions on*, vol. PP, no. 99, 2015.
- [24] V. Cirimele, F. Freschi, and P. Guglielmi, "Wireless power transfer structure design for electric vehicle in charge while driving," in *Electrical Machines (ICEM), 2014 International Conference on*, pp. 2461–2467, 2014.
- [25] J. Sallan, J. Villa, A. Llombart, and J. Sanz, "Optimal design of ICPT systems applied to electric vehicle battery charge," *Industrial Electronics, IEEE Transactions on*, vol. 56, no. 6, pp. 2140–2149, 2009.
- [26] C.-S. Wang, G. A. Covic, and O. H. Stielau, "Power transfer capability and bifurcation phenomena of loosely coupled inductive power transfer systems," *IEEE Transactions on Industrial Electronics*, vol. 51, pp. 148–157, Feb 2004.